

Muonium depolarization by electron spin exchange with O₂ gas in the temperature range 90–500 K

Masayoshi Senba, Donald G. Fleming, Donald J. Arseneau,
David M. Garner, and Ivan D. Reid*

TRIUMF and Department of Chemistry, University of British Columbia, Vancouver, British Columbia, Canada V6T 1Y6

(Received 25 August 1988)

The thermally averaged depolarization cross sections, $\bar{\sigma}_D(T)$, for Mu+O₂ electron spin exchange, have been measured by the muon spin relaxation (μ SR) technique in a N₂ moderator at total pressures near 1 atm over the temperature range 88–500 K. These values are related to the thermal spin-flip cross sections of interest ($\bar{\sigma}_{SF}$) by a simple numerical factor. At temperatures $\gtrsim 120$ K, $\bar{\sigma}_D(T)$ is essentially temperature independent [with $\bar{\sigma}_{SF}=(5.7\pm 0.5)\times 10^{-16}$ cm²], though exhibiting a slight tendency to increase with temperature. At lower temperatures, $\bar{\sigma}_{SF}(T)$ decreases noticeably. Comparison with the only currently available theoretical calculations of Mu(H)+O₂ spin-flip cross sections by Aquilanti, Grossi, and Laganà [Hyperfine Interact. **8**, 347 (1981)] on the potential-energy surface of Farantos *et al.* [Mol. Phys. **34**, 947 (1977)] gives poor agreement with the data, particularly in their temperature dependence. The present results for $\bar{\sigma}_{SF}(T)$ for Mu+O₂ qualitatively exhibit the same trend with temperature as found by Desaintfuscién and Audoin [Phys. Rev. A **13**, 2070 (1976)] for H-H spin exchange over a comparable temperature range, but the H-H cross sections are, surprisingly, about four times larger. Comparisons with the experimental H+O₂ spin-exchange cross sections of Anderle *et al.* [Phys. Rev. A **23**, 34 (1981)] and of Gordon *et al.* [JETP Lett. **17**, 395 (1973)], indicate a significant isotope effect, with $\bar{\sigma}_{SF}(H)\gtrsim 1.5\bar{\sigma}_{SF}(\text{Mu})$. While this effect can be qualitatively understood in terms of the differing numbers of partial waves involved, detailed theoretical calculations on more recent potential-energy surfaces for HO₂ are called for.

I. INTRODUCTION

In the realm of gas-phase collision phenomena, electron spin exchange at thermal energies can be regarded as a quasielastic process in which the total spin S of the colliding partners is conserved, but their spin projection quantum numbers are “exchanged” as a result of scattering from a spin-dependent potential $V(\mathbf{r}, \mathbf{R})\mathbf{S}_1\cdot\mathbf{S}_2$ (Refs. 1–3), where \mathbf{R} is the internuclear displacement in the molecule and \mathbf{r} is the atom-molecule displacement. For a given partial wave, the spin-exchange cross section is due to a spin-flip process (σ_{SF}), determined by the difference in phase shifts for different total spins.

Although well studied in optical pumping experiments, particularly those involving collisions of the alkali metals,^{2–4} there are relatively few experimental reports of electron spin exchange between a H atom and a paramagnetic atom or molecule.^{5–8} Moreover, unlike reactive scattering studies of the H atom, where isotopic substitution, including recently that of muonium (Mu = μ^+e^-),^{9–12} continues to play an important role, there are only a few measurements of the effects of isotopic mass substitution on electron spin exchange.² Although work is in progress, to our knowledge there has as yet been no direct comparison of H and D atom spin exchange.¹³ Muonium is produced 100% spin polarized and consequently may be a facile probe of electron spin exchange at thermal energies, utilizing the muon-spin-relaxation (μ SR) technique^{9–12} to sensitively monitor the shared muon and electron spin polarization with time.

Moreover, comparison of Mu and H is more likely to reveal the effect, if any, of isotopic mass substitution on H-atom spin-exchange cross sections, due to the unparallel mass difference between these two atomic species ($m_\mu = \frac{1}{9}m_p$). Indeed, in the case of H-H collisions, theory¹⁴ predicts that the low-energy spin-exchange cross section for Mu-H should be enhanced by an order of magnitude over H-H, due to resonant capture.

The Mu-H experiment has not yet been attempted, but the corresponding experimental studies of H-H spin exchange⁶ give exemplary agreement with theory over a wide range of temperatures.¹⁵ Resonant enhancement of $\sigma_{SF}(E)$ at low energies for Mu-O₂ over that for H-O₂ has also been predicted,¹⁶ using a semiempirical potential (energy surface) for the H-O₂ interaction.¹⁷ Unfortunately, in contrast to the essentially exact calculations for atomic Mu-H and H-H spin exchange,^{14,15} uncertainties in the atom-molecule potential compromise the accuracy in calculations of $\sigma_{SF}(E)$ for H(Mu)-O₂ spin exchange. Moreover, for nonspherical particles, the exchange interaction is orientation dependent, and changes during a collision due to rotation, further complicating the calculation of molecular spin-exchange cross sections.

The semiempirical calculations indeed gave poor agreement with previously published experimental results for both H+O₂ (Refs. 5, 7, and 8) and Mu+O₂ spin exchange in the temperature range ~ 300 –500 K.^{18,19} On the other hand, they did demonstrate that Mu can be a much more sensitive probe of the anisotropic nature of the interaction than H-atom spin exchange can. Such

effects are pronounced at lower temperatures, where resonant enhancements in $\sigma_{\text{SF}}(E)$ for $\text{Mu} + \text{O}_2$ are naturally manifest, a situation that prompted the present study of $\text{Mu} + \text{O}_2$ to temperatures below 90 K. A preliminary report of this work has been given elsewhere.¹⁹ In the present paper we have extended these studies, obtaining more low-temperature data points, as well as repeating those obtained earlier at higher (≥ 300 K) temperatures.¹⁸

Finally, it can be remarked that since the 1981 theoretical calculations comparing the H-O_2 and Mu-O_2 systems,¹⁶ additional *ab initio*^{20–22} as well as semiempirical²³ potentials for H-O_2 have been reported. Those in Refs. 20 and 21 in particular give reasonably good accounts of both the reactive cross sections and rovibrational partitioning seen in reactive scattering.²⁴ It is hoped that the present results for Mu-O_2 spin exchange will prompt further theoretical calculations of $\sigma_{\text{SF}}(\text{Mu})$ and $\sigma_{\text{SF}}(\text{H})$ on these newer potential surfaces.

II. SPIN EXCHANGE AND μSR

A. The transverse-field μSR technique

The positive muon is produced 100% longitudinally spin polarized at MeV kinetic energies. During its slowing down processes in a moderating gas such as N_2 , muonium ($\text{Mu} = \mu^+ e^-$) is formed repeatedly through a series of rapid charge-exchange cycles beginning at keV energies, with stable Mu emerging at kinetic energies $\lesssim 20$ eV,²⁵ depending on the ionization potential of the moderator. Thermalization to $k_B T$ energies then takes place by elastic and inelastic scattering and takes about 10 ns in N_2 at 1 atm pressure. Classically, in a weak transverse magnetic field ($\lesssim 10$ G), the μ^+ and e^- spins are coupled by the muon-electron hyperfine interaction such that triplet muonium ($F=1, M=1$) precesses with a characteristic Larmor frequency, whereas muonium in its singlet state ($F=0, M=0$) does not precess at all. Here (F, M) are the usual hyperfine quantum numbers. At observation times, after thermalization, the initial polarization is seen to be shared between muons in muonium (P_{Mu}) and those in diamagnetic environments (P_D). Another possibility, the formation of muonated radicals,¹¹ is not relevant here. Some depolarization takes place during the slowing down process due to hyperfine mixing, manifest as a “lost” fraction (P_L), which is strongly moderator-pressure dependent. At ~ 1 atm N_2 though, $P_L=0$ and will not be considered further. See discussions in Ref. 25. It is known that $P_{\text{Mu}}=0.85$ and $P_D=0.15$ in N_2 at pressures ≥ 1 atm, so that most muons thermalize as muonium.²⁵ The actual diamagnetic species is likely the N_2Mu^+ molecular ion.^{9,25}

Since in the decay of the μ^+ ($\mu^+ \rightarrow e^+ \nu_e \bar{\nu}_\mu$) the decay positron is emitted preferentially along its spin direction, a counter array set at a fixed angle will record an oscillating decay pattern as the μ^+ spin sweeps past. The time difference between the detection of an incident μ^+ and its decay positron is incrementally recorded, defining a μSR histogram of $\sim 10^6$ events. In the present experiments, positrons were recorded in two separate counter telescopes, positioned at either 90° and 270° or 0° and 180°

with respect to the incident μ^+ spin, the latter geometry in the case of a spin-rotated muon beam.²⁶ For most runs the magnetic field was set to ~ 8 G in order to measure coherent Mu precession (ω_{Mu}). In such weak fields, the μSR histogram “signal” $S(t)$ can be written in the form

$$S(t) = P_{\text{Mu}} e^{-\lambda t} \cos(\omega_{\text{Mu}} t + \phi_{\text{Mu}}) + P_D \cos(\omega_D t - \phi_D), \quad (1)$$

where ω_{Mu} and ω_D are the Larmor frequencies of Mu and diamagnetic muons, respectively, and ϕ_{Mu} and ϕ_D are their initial phases. Muonium precession is easily distinguished from those muons precessing in diamagnetic environments ($\omega_{\text{Mu}} = 103\omega_D$). The quantity of principal interest in these experiments is the relaxation rate λ , which reflects the interaction of the Mu spin with its environment.

Figure 1 presents typical μSR signals $S(t)$ for Mu in N_2 gas both in the absence [Fig. 1(a)] and presence [Fig. 1(b)] of trace amounts of added O_2 gas. The solid lines are fits of Eq. (1) to the data from which the quantities of general interest (P_{Mu} , P_D , and λ) can be extracted. The dramatic increase seen in relaxation rate λ in the signal shown in Fig. 1(b), obtained in the presence of 270 ppm

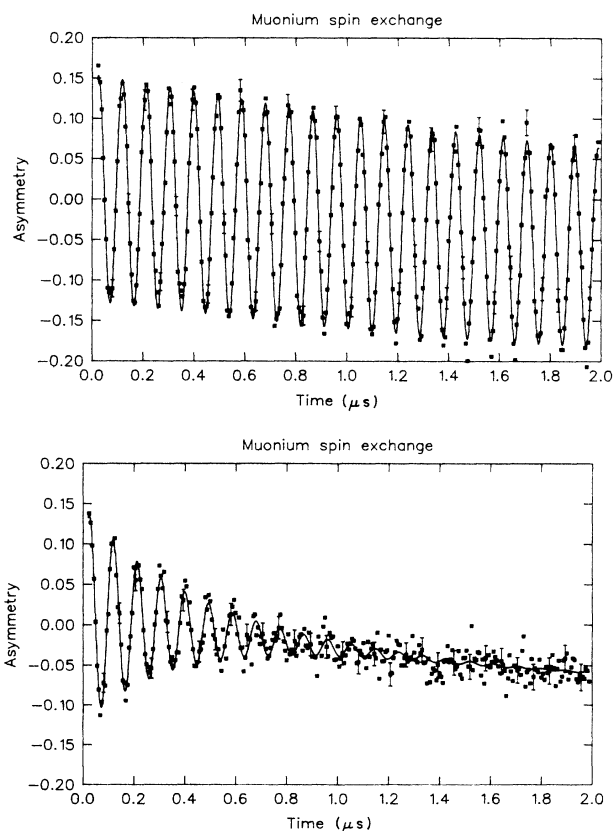


FIG. 1. The μSR signals $S(t)$ at 100 K for coherent Mu precession in a magnetic field of 8 G in pure N_2 at 800 Torr pressure (a) and in N_2 doped with 270-ppm O_2 (b). The solid line is a fit of Eq. (1) to the data. Note the pronounced increase in relaxation rate (λ) in the signal in (b), due to spin-exchange collisions of Mu with O_2 .

of O_2 , is obvious. This is due to electron spin exchange, as discussed further below. In both cases, in the weak fields used, the small diamagnetic signal ($P_D=0.15$) develops only about $\frac{1}{2}$ cycle of precession on the time scale of Fig. 1, giving the appearance then of an underlying "distortion" in the data, which must be properly accounted for in the analysis [the second term of Eq. (1)].

The correct quantum-mechanical treatment leading to the classical picture described above has been given in detail elsewhere,^{27,28} but is highlighted here as well because it provides the necessary basis for understanding the effect of spin exchange on the muon polarization. The initial-state vectors for the Mu atom, quantized along the original μ^+ -spin direction, can be written as an equal population of $|A\rangle_{\parallel} = |\alpha_{\mu}\alpha_e\rangle$ and $|B\rangle_{\parallel} = |\alpha_{\mu}\beta_e\rangle$, reflecting the fact that the muon is polarized (α_{μ}), but the electron is not. In zero or in a longitudinal magnetic field, $|A\rangle_{\parallel} = |11\rangle$ is an eigenstate of the Hamiltonian. The $|B\rangle_{\parallel}$ state, however, is not an energy eigenstate (except in a strong longitudinal field), and oscillates between the $|10\rangle$ and $|00\rangle$ eigenstates at the μ^+e^- hyperfine frequency ($\nu_0=4463$ MHz). Thus the $|B\rangle_{\parallel}$ state appears effectively depolarized because our experimental time resolution is typically $\gtrsim 1$ ns. Hence the observed polarization of the muon ensemble in zero field is half its maximum value.

This can easily be seen from the full density matrix of both $|A\rangle_{\parallel}$ and $|B\rangle_{\parallel}$ states, expressed in terms of the eigenstates of the (zero-field) Hamiltonian.^{27,28} We write

$$\begin{aligned} \rho_{\text{Mu}} &= \frac{1}{2} |\alpha_{\mu}\alpha_e\rangle \langle \alpha_{\mu}\alpha_e| + \frac{1}{2} |\alpha_{\mu}\beta_e\rangle \langle \alpha_{\mu}\beta_e| \\ &= \frac{1}{2} |11\rangle \langle 11| + \frac{1}{4} |10+00\rangle \langle 10+00|. \end{aligned} \quad (2)$$

Equation (2) evolves in time according to

$$\begin{aligned} \rho_{\text{Mu}}(t) &= \frac{1}{2} |11\rangle \langle 11| + \frac{1}{4} [|10\rangle \langle 10| + |00\rangle \langle 00|] \\ &\quad + \frac{1}{4} (e^{+i\omega_0 t} |10\rangle \langle 00| + e^{-i\omega_0 t} |00\rangle \langle 10|). \end{aligned} \quad (3)$$

The last two terms in Eq. (3) oscillate at the hyperfine frequency ($\omega_0=2\pi\nu_0$), and are averaged to zero by the experimental time resolution. In zero (or longitudinal) magnetic field, the (time-independent) muon polarization in Mu is then defined by

$$P_{\text{Mu}}^{(t)} = \langle \sigma_z^{\mu} \rangle = \text{Tr} \sigma_z^{\mu} \rho_{\text{Mu}}^{(t)} = \frac{1}{2} \text{Tr} |\alpha_{\mu}\alpha_e\rangle \langle \alpha_{\mu}\alpha_e| = \frac{1}{2}, \quad (4)$$

since σ_z^{μ} operating on the second term in Eq. (3) gives identically zero by orthogonality. Equation (4) assumes the initial beam polarization is 100%. In a longitudinal magnetic field (H), the final result is only slightly more complicated,

$$P_{\text{Mu}}(X) = \frac{1}{2} \left[1 + \frac{X^2}{1+X^2} \right], \quad (5)$$

where $X = H/H_0$, with $H_0 = 1585$ G, the contact field of the μ^+ at the electron.²⁷ This result was first derived some years ago by Mobley²⁹ and indicates, in general, that the experimental depolarization cross section will be field dependent.

In a transverse (\perp) magnetic field, neither $|A\rangle_{\perp}$ nor

$|B\rangle_{\perp}$ are energy eigenstates. They can be expressed, however, as a superposition of Zeeman eigenstates and correspondingly evolve in time with a characteristic response of four distinct frequencies (ω_{12} , ω_{23} , ω_{14} , and ω_{34}), given by the usual selection rules, $\Delta F=1$, $\Delta M=\pm 1$.^{27,28} In a transverse field, the muon polarization can be found from the expression

$$P_{\perp}^{\mu}(t) = \frac{1}{2} \langle A_{\perp}(t) | \sigma_z^{\mu} | A_{\perp}(t) \rangle + \frac{1}{2} \langle B_{\perp}(t) | \sigma_z^{\mu} | B_{\perp}(t) \rangle. \quad (6)$$

In a weak transverse field, Eq. (6) can be shown^{27,28} to have the form

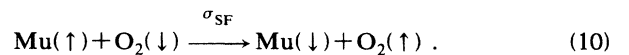
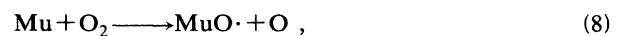
$$P_{\perp}^{\mu}(t) = \frac{1}{4} [(e^{i\omega_{12}t} + e^{i\omega_{23}t}) + (e^{-i\omega_{34}t} + e^{i\omega_{14}t})]. \quad (7)$$

In the particular case of interest here, for fields $\lesssim 10$ G, the frequencies ω_{12} and ω_{23} originate almost exclusively from the original $|A\rangle_{\parallel}$ state, whereas ω_{34} and ω_{14} originate from the $|B\rangle_{\parallel}$ state. Since the latter two angular frequencies are both comparable to $\omega_0=2\pi\nu_0$, they are again averaged to zero by the ~ 1 -ns experimental time resolution, leaving the now essentially degenerate frequencies ω_{12} and ω_{23} . These then give rise to the experimentally observable coherent muonium precession signal, $P_{\perp}(t) = \frac{1}{2} e^{i\omega_{\text{Mu}}t}$ from Eq. (7).

The initial amplitude (P_{Mu}), however, is usually different from $\frac{1}{2}$ since it depends on a number of other factors. In addition, an exponential relaxation rate (λ) is introduced to account for the time dependence of this amplitude, thus accounting for the first term of the μSR signal $S(t)$ in Eq. (1), expressed as the real part of $P_{\perp}(t)$. The second term of Eq. (1), coming from contributions due to muons in diamagnetic environments, follows trivially because the time dependence of this part of the ensemble is simply $e^{-i\omega_D t}$, again with the initial amplitude P_D determined empirically. Relaxation of the diamagnetic part of the signal is not measurable at the ~ 8 -G fields of interest.

B. Muonium spin exchange (with O_2)

In analogy with magnetic resonance, random encounters in the gas that serve to perturb the triplet Mu state give rise to spin relaxation, which, in the case of a transverse field, can be thought of as a dephasing ($\lambda=1/T_2$) process. It can be remarked that T_2 is of order $1 \mu\text{s}$ in our experiments, orders of magnitude longer than the ~ 10 -ns thermalization time of the muon;²⁵ i.e., relaxation is a measure of a *thermal* rate process. There are in principle three reactions that could give rise to spin dephasing of the Mu ensemble in the case of $\text{Mu} + O_2$, all of which actually result in paramagnetic environments for the muon:



Reaction (8) is ~ 17 kcal/mol endothermic and could not measurably contribute to thermal relaxation rates at

the temperatures of interest here. This reaction likely occurs at epithermal (hot atom) energies though, since appreciable cross sections in the few-eV range have been reported in the corresponding H-atom studies.²⁴ The second reaction forms the muon analog of the hyperoxy radical which, as indicated, requires a third body (M) stabilizing collision. The pressure dependence of the corresponding H-atom addition reaction has been studied, and lifetimes (τ_c) for the unimolecular (RRKM) dissociation have been estimated;^{24,30} for low J states, $\tau_c \lesssim 1$ ps is expected, corresponding to the observation of high-pressure-limiting rate constants at pressures of ~ 200 bars. At the low (~ 1 bar N_2) pressures of the present experiment, the reaction is third order. Relaxation rates λ for the formation of MuO_2 at the 1 Torr O_2 partial pressure used, estimated from the H-atom addition rates recently reported in Ref. 30, are typically $\lesssim 0.01\lambda_0$, far too slow to contribute. This assessment is entirely consistent with earlier estimates of the same process.¹⁸ Hence the only reaction of interest here is the spin-exchange one (10) under discussion.

A fourth possibility can be noted: intermolecular dipole-dipole relaxation. However, this is discounted since the strength of the Heisenberg exchange splitting is typically 100-fold greater than that of the dipole-dipole interaction, as evidenced, for example, in calculations of the energy levels of the spin-dependent O_2 - O_2 interaction in the gas phase.³¹ An alternative argument lies in the strength of the corresponding magnetic field, estimated to be ~ 1 kG at a distance ~ 1 Å. Assuming an interaction time $\tau \sim 10^{-13}$ s, corresponding to the motion of a thermal Mu atom past an O_2 molecule, the amount of dephasing ($\phi = \omega_{Mu}\tau$) is $\sim 10^{-4}$ rad per collision. Even at the maximum O_2 concentration in the present experiment (see Fig. 2), there are only $\sim 10^7$ collisions/s, which in a total measurement time of say 4 μ s would correspond to a maximum dephasing of only 0.004 rad, far too small to cause any relaxation.

In a weak transverse magnetic field, there is a predictable phase coherence between the three magnetic substates of triplet Mu: $|11\rangle = |\alpha_\mu\alpha_e\rangle$, $|10\rangle = (1/\sqrt{2})(|\alpha_\mu\beta_e + \beta_\mu\alpha_e\rangle)$, and $|1-1\rangle = |\beta_\mu\beta_e\rangle$. Spin-exchange encounters in the gas at random times cause depolarization, and hence relaxation (dephasing) of the μ SR signal. For purposes of illustration, however, consider the situation in *zero* field, first in the case of Mu spin exchange with a single unpaired electron (e.g., $Mu + NO$, as in Ref. 18). For a given electron pair ($Mu \cdot NO$), electron exchange can be represented by the operator $P_{12} = \frac{1}{2}(1 + \sigma_1 \cdot \sigma_2)$, where σ_1 and σ_2 are the usual Pauli spin operators. Thus $P_{12}|\alpha\beta'\rangle = |\beta\alpha'\rangle$ causes "spin flip," but $P_{12}|\alpha\alpha'\rangle = |\alpha\alpha'\rangle$ effects no change, although it could be thought of as an exchange of like spins. Since the NO is unpolarized, the two initial states of the two-electron system, $|\alpha_\mu\alpha\alpha'\rangle$ and $|\alpha_\mu\alpha\beta'\rangle$, would be equally populated. The initial density matrix for the $Mu \cdot NO$ system then has the form [recall Eqs. (2) and (4)]

$$\rho_{Mu}^i = \frac{1}{4}|\alpha_\mu\alpha\alpha'\rangle\langle\alpha_\mu\alpha\alpha'| + \frac{1}{4}|\alpha_\mu\alpha\beta'\rangle\langle\alpha_\mu\alpha\beta'|. \quad (11)$$

In a purely elastic encounter there is no change in these

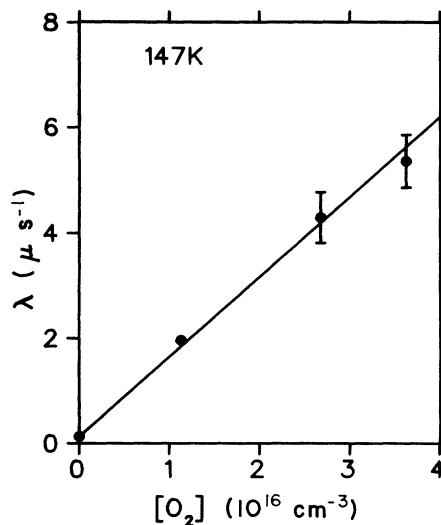


FIG. 2. A plot of relaxation rate (λ) vs O_2 concentration for the spin-exchange scattering of $Mu + O_2$ at 147 K. These data were taken in the presence of added Al foil (see Table I). The straight line is a χ^2 fit of Eq. (16) to the data. The slope gives the depolarization rate constant of interest, $k_D = 1.56 \times 10^{-10} \text{ cm}^3 \text{ s}^{-1}$. Error bars are statistical only.

states, but the scattering interaction is also spin dependent,^{1,2} which can be written in a form exhibiting the exchange operator P_{12} ,

$$V_{\text{int}}(r) = V_C(r) + V_S(r)(1 + \sigma_1 \cdot \sigma_2), \quad (12)$$

where $V_C(r)$ is dominated by a Coulomb-like interaction, and V_S , also Coulomb-like, is the strength of the spin-dependent part of the potential. After a spin-exchange scattering, $|\alpha_\mu\alpha\alpha'\rangle$ in Eq. (11) is unchanged, but the other half of the ensemble changes to $|\alpha_\mu\beta\alpha'\rangle$. Tracing over the unpolarized NO states (α' , β') gives the new Mu density matrix,

$$\rho_{Mu}^f = \frac{1}{4}|\alpha_\mu\alpha\rangle\langle\alpha_\mu\alpha| + \frac{1}{4}|\alpha_\mu\beta\rangle\langle\alpha_\mu\beta|. \quad (13)$$

Spin flip causes depolarization for exactly the same reason as defined by Eq. (2) above; i.e., $|\alpha_\mu\beta\rangle = (1/\sqrt{2})(|10\rangle + |00\rangle)$, and this superposition of eigenstates again depolarizes the muon on a time scale of the hyperfine interaction, 0.2 ns. On average, each such spin-exchange collision with unpolarized NO depolarizes half the muon ensemble. It is important to note that the time between depolarizing collisions is much longer than this hyperfine mixing and muon-electron recoupling time; $\gtrsim 0.1 \mu$ s at the low (O_2) partial pressures in the experiment. Moreover, the loss of muon polarization is irreversible: even if $|\alpha_\mu\beta\rangle$ were to convert back to $|\alpha_\mu\alpha\rangle$ in a subsequent encounter, this would have completely lost phase coherence with the original ensemble. In this regard, μ SR is fundamentally different from H-atom maser or atomic-beam studies,^{5,7,8} where state selected populations or population differences are monitored directly.

The situation in collisions of Mu with O_2 is more complicated than with NO because $Mu \cdot O_2$ is a three-electron

system, but one can define an exchange operator for each pair and an overall exchange operator for the combined system by

$$P_{\text{Mu-O}_2} = P_{12} + P_{13} = \frac{1}{2}[2 + \sigma_{\text{Mu}} \cdot \sigma_{\text{O}_2}(2,3)], \quad (14)$$

where electrons labeled as (2,3) are associated with the O₂ molecule. The O₂ is again unpolarized, with only its ground ($S=1$) state populated at room temperature (the Σ_g^+ state lies at ~ 1 eV and can be ignored). In Eq. (14), $\sigma_{\text{O}_2} = 2S_{\text{O}_2}$ is defined like the Pauli spin operator for $S = \frac{1}{2}$, and operates on the appropriate column vector for $S=1$. It can be noted that the exchange interaction defined in this way is zero for spin-0 molecules. The interaction operator $\sigma_{\text{Mu}} \cdot \sigma_{\text{O}_2}$ has a 9×9 matrix representation with both the exchange of like and unlike spins giving nonzero matrix elements, but only spin-flip exchange contributes to relaxation of the μSR signal.

For example, consider again the zero-field density matrix for Mu colliding with equal probability with unpolarized O₂ in *gedanken* $|11'\rangle$ and $|1-1'\rangle$ states (primes denote electrons coming from the O₂ and, for simplicity, the $|10'\rangle$ state is ignored here). Before scattering, the initial density matrix of this hypothetical system can be written in the form

$$\rho^i = \frac{1}{4}|\alpha_\mu\alpha\alpha'\rangle\langle\alpha_\mu\alpha\alpha'| + \frac{1}{4}|\alpha_\mu\alpha\beta'\rangle\langle\alpha_\mu\alpha\beta'|, \quad (15)$$

which has the same initial polarization of $\frac{1}{2}$ as defined by Eq. (4) or Eq. (11). After spin exchange with each O₂ electron and tracing over unpolarized O₂, the final Mu density matrix has the same form as given in Eq. (13), so that again half of the initial polarization is lost with each such encounter. In reality, the present experiments have been carried out in a transverse field and each of the magnetic substates of the coherently precessing Mu atom must be considered, as well as the $|10'\rangle$ state of the unpolarized O₂ molecule. This modifies the simple factor of $\frac{1}{2}$, as shown below (although it remains correct for NO). It is recalled that in weak fields the experimental precession signal, $P_\perp(t)$, can be identified with the original Mu triplet state, $|A\rangle_\parallel = |\alpha_\mu\alpha_e\rangle$. Thus the $|11\rangle = |\alpha_\mu\alpha_e\rangle$ zero-field case discussed above is one such substate in a full treatment of the density matrix of Mu spin exchange in a transverse field of arbitrary strength.³²

On average, if one considers all possible encounters of (precessing) Mu and freely tumbling unpolarized O₂ (or NO) in the gas, the exchange of like and unlike spins is equally likely, but only spin-flip processes actually lead to depolarization, in either a transverse or longitudinal (or zero) magnetic field environment.^{29,32} This conclusion appears to be at variance with a similar treatment some time ago by Ferrell on positronium-atom ($\text{Ps} = e^+e^-$) spin exchange, where both the exchange of like and unlike spins were considered as contributing equally to triplet-singlet conversion in Ps annihilation.³³ In a bulk kinetic experiment such as the present one, we are not able to identify the individual cross sections that give rise to depolarization, measuring instead only the combined effect of these spin-exchange collisions, as manifest by the

“depolarization” rate λ_D . This can be defined experimentally by

$$\lambda = \lambda_0 + \lambda_D = \lambda_0 + k_D n_{\text{O}_2}, \quad (16)$$

where λ_0 is some background relaxation in the pure (N₂) moderator, and k_D is the corresponding bimolecular rate constant, with n_{O_2} being the number density of oxygen added to the moderator. As discussed further below, this rate constant is easily related to the spin-flip cross section σ_{SF} , which can be calculated theoretically.^{1-3,14,15} The background relaxation rate could be due to magnetic field inhomogeneities or to chemical or even spin-exchange encounters with residual impurities in the N₂. Usually, as in the present case, $\lambda \gg \lambda_0$, so that the magnitude and origin of λ_0 is not a concern (see, however, Ref. 10). It is noted that the data-acquisition logic dictates that there be only *one* Mu atom in the system at a time, so that there is no possibility, for example, of Mu-Mu spin-exchange encounters.

III. EXPERIMENT

A. Apparatus

The experiments were carried out at the TRIUMF cyclotron, a meson facility on the campus of the University of British Columbia. A 15-l aluminum target vessel designed^{19,34} to allow temperature variation by hot or cold air flow, was positioned in the center of a 1.5-m-diam Helmholtz coil, which provided the necessary magnetic field. Over a stopping volume of ~ 1 l, the field was homogeneous to $\sim 0.1\%$. The temperature could easily be varied in the range ~ 90 – 500 K by a variable flow of compressed air first passed through an appropriate heat exchanger [a ceramic heater for temperatures > 300 K, and a liquid-nitrogen (LN) Dewar for temperatures < 300 K], which then flowed over the inside reaction cylinder. Temperature homogeneity in the reaction cylinder was constantly monitored by thermocouples that could be moved along its length; typically, the temperature was constant in the reaction region over the course of the experiment to better than ± 5 K, being most stable at the higher temperatures (Table I). High-purity (reagent-grade) O₂ was used directly from the lecture bottle without further purification. A small (110 cm³) standard volume was first pressurized with O₂ to ~ 100 Torr and then discharged into the previously evacuated target vessel, which was then pressurized with N₂ to a total pressure in the range ~ 300 – 1100 Torr. Absolute O₂ pressures in the standard volume were measured with an MKS Baratron capacitance manometer and are believed accurate to $\pm 1\%$ or better. Typical O₂ partial pressures in the reaction vessel were of the order 0.1 Torr, calculated from the ideal-gas law, and usually four different partial pressures (concentrations) were run at a given temperature and total pressure in order to establish the bimolecular rate constant [Eq. (16)].

Several off-line tests of pressure and temperature variation were carried out to ascertain the importance of adsorption and/or (O₂)₂ dimer formation,^{31,35} since we had

TABLE I. Depolarization rate constants (k_D) and thermally averaged cross sections [$\bar{\sigma}_D(T)$] for $\text{Mu} + \text{O}_2$ spin exchange: (a) obtained in an unperturbed target vessel and (b) obtained in the presence of fivefold increase in Al surface area.

T (K)	Pressure (Torr)	k_D (10^{-10} s^{-1})	$\bar{\sigma}_D(T)$ (10^{-16} cm^2)
(a) Unperturbed target vessel			
88(7)	430 (N_2)	1.19(4)	2.93(10)
100(5)	800 (N_2)	1.27(4)	2.93(9)
108(6)	450 (N_2)	1.30(4)	2.87(9)
118(5)	800 (N_2)	1.42(5)	3.02(11)
128(6)	800 (N_2)	1.66(6)	3.39(12)
135(5)	525 (N_2)	1.72(5)	3.42(10)
176(3)	575 (N_2)	1.93(6)	3.36(10)
188(4)	800 (N_2)	1.97(4)	3.32(7)
217(4)	700 (N_2)	2.17(8)	3.40(13)
295(5)	800 (N_2)	2.64(41)	3.55(55)
295(5)	800 (Ar)	2.50(20)	3.36(26)
296(2)	1070 (N_2)	2.57(8)	3.45(11)
296(2)	800 (N_2)	2.68(16)	3.60(21)
338(2)	800 (N_2)	2.83(21)	3.55(26)
405(2)	800 (N_2)	3.25(21)	3.73(24)
500(2)	800 (N_2)	3.61(26)	3.73(27)
(b) Fivefold increase in Al surface area			
100(5)	800 (N_2)	1.21(3)	2.79(7)
100(6)	400 (N_2)	1.12(5)	2.58(12)
123(4)	800 (N_2)	1.47(4)	3.06(8)
130(4)	800 (N_2)	1.51(4)	3.06(8)
147(3)	300 (N_2)	1.56(7)	2.87(13)
200(5)	400 (N_2)	2.07(8)	3.38(13)
298(2)	600 (N_2)	2.78(10)	3.72(13)

previously seen a rather sharp ($\approx 15\%$) decrease in k_D at temperatures $\lesssim 110 \text{ K}$,¹⁹ indicative of a physical artifact such as surface adsorption rather than of Mu interactions in the gas. At a low (~ 30 torr) total pressure of O_2 , the ratio P/T was found to be constant and reproducible for temperatures from ~ 110 to 85 K , with the temperature itself controlled to $\pm 1^\circ$, or better. A similar measurement at a total pressure of 800 Torr gave fluctuations in the initial values of P/T , likely due to O_2 condensation on a cold spot near the cold (LN) inlet line, but which again recovered to a constant value at temperatures $\gtrsim 110 \text{ K}$, although a few-percent decrease was seen at temperatures below 110 K . It can also be noted that no change in pressure was found at room temperature at any O_2 or $\text{O}_2\text{-N}_2$ pressure. In order to change the surface area of the target vessel, Al foil was inserted throughout its interior, effecting an approximately fivefold increase. Measurements over the temperature range $110\text{--}300 \text{ K}$ with pure N_2 at 800 Torr again gave little or no change in P/T , but in the case of a 10% O_2 mixture, at 800 Torr total pressure, there did appear to be an $\sim 5\%$ decrease in the ratio P/T at temperatures near 100 K ; this was, however, much less than the total change that could be expected on the basis of the change in surface area. Moreover, repeating these measurements at ~ 30 Torr O_2 total pressure revealed no change in the ratio P/T , regardless of the amount of Al foil present. It is noted that the mass of

adsorbed gas, either N_2 or O_2 , to form a monolayer on an Al_2O_3 surface is estimated to be $\sim 5.3 \text{ g/cm}^2$,³⁶ which would cause only about a 1% change in O_2 partial pressure at the conditions of our experiment.

Since we feel that a change in absolute pressure could certainly be measured to better than the 5% level, which is the maximum effect seen, these off-line tests indicate that the formation of O_2 dimers and/or O_2 surface adsorption (perhaps enhancing dimer formation) at low temperatures cannot be higher than this level. It is noted that the formation of gas-phase O_2 dimers is only likely at temperatures $\lesssim 100 \text{ K}$.³⁵ Although seemingly unlikely, the possibility of preferential O_2 adsorption in the presence of a large amount of N_2 should also be considered.

B. Results

Figure 2 presents a plot of λ versus $[\text{O}_2]$ taken at 147 K in a magnetic field of 7.5 G . These data were actually obtained in the presence of added Al foil (Table I), but are typical over the whole range of experimental conditions studied. The straight line is a least-squares fit of Eq. (16) to the data, yielding the depolarization rate constant from the slope, $k_D = 1.56(7) \times 10^{-10} \text{ cm}^3 \text{ s}^{-1}$. The corresponding thermally averaged depolarization cross section $\bar{\sigma}_D(T)$ can be obtained from the definition

$$k_D(T) = \left[\frac{8k_B T}{\pi\mu} \right]^{1/2} \left[\frac{1}{k_B T} \right]^2 \int_0^\infty \sigma_D(E) E e^{-E/k_B T} dE$$

$$= \overline{v(E)\sigma_D(E)} = \bar{v}_{(T)} \bar{\sigma}_D(T) = \bar{v} \bar{\sigma}_D, \quad (17)$$

where $\sigma_D(E)$ represents the energy-dependent total cross section and $\bar{v} = (8k_B T/\pi\mu)^{1/2}$ is the relative velocity of colliding partners; for the data in Fig. 2, $\bar{\sigma}_D(T) \equiv \bar{\sigma}_D = 2.87(13) \times 10^{-16} \text{ cm}^2$ at 147 K . Here, the overbar denotes a thermal average and the notation $\bar{\sigma}_D(T)$ serves as a reminder that the thermally averaged cross sections are temperature dependent. Table I presents our results for both $k_D(T)$ and $\bar{\sigma}_D(T)$ for the range of temperatures and moderator pressures studied. The table is divided into two parts: entries in part (a) were all obtained in an unperturbed target vessel; those in part (b) were obtained in the presence of a fivefold increase in Al surface area, in the manner described above. Several entries are given at room temperature, showing the reproducibility in the data, which agrees well also with earlier reported values in different moderators and over a range of higher temperatures.¹⁸ It is noted, though, that the present data are generally characterized by much smaller error bars.

From Eq. (17) it can be seen that if the depolarization cross section is independent of energy, then a plot of $k_D(T)$ versus $T^{1/2}$ should yield a straight line; more generally, $\log k_D(T)$ versus $\log T$ gives the slope n . On such a plot (not shown), the data from Table I fall naturally on two separate lines, defined by the temperature intervals $88\text{--}120$ and $\sim 120\text{--}500 \text{ K}$, but with slopes $n = 0.55 \pm 0.03$ in both intervals, indicating a minimal temperature dependence in the underlying spin-exchange cross sections.¹⁹ Figure 3 shows a plot of the thermally averaged cross sections $\bar{\sigma}_D(T)$ versus T , over the full temper-

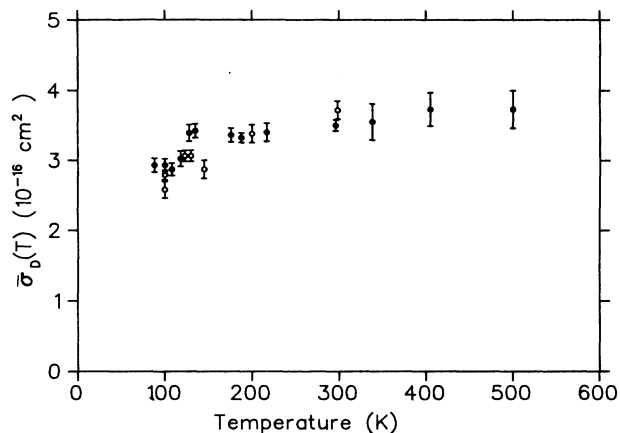


FIG. 3. The experimentally determined depolarization cross sections $\bar{\sigma}_D(T)$ obtained from the thermal rate constants $k_D(T)$ vs temperature (K). The solid circles were obtained in an unperturbed Al target vessel, while the open circles were obtained in the presence of added Al foil, which increased the surface area of the target by about fivefold. Several room-temperature points have been combined (see Table I).

ature range of the data in Table I. The solid points are entries from part (a) of this table; the open ones are from part (b) (i.e., those obtained in the presence of added Al foil). In both cases, total pressure variations in the range ~ 300 – 800 Torr at temperatures ~ 100 K are represented (Table I). Like the rate constants themselves, the thermal cross sections appear to exhibit two distinct temperature intervals, with slightly increasing values within each interval. The apparent step decreases seen in $\bar{\sigma}_D(T)$ at ~ 120 K in the absence of added Al foil and, at ~ 140 K in the presence of this foil, if real, could be due to surface effects on the O_2 concentration, as discussed below. In both cases, though, this step is predicated on only one data point and we are inclined to the view that the data represent a fairly smooth but modest decrease in $\bar{\sigma}_D(T)$ for $T \lesssim 120$ K.

There are three conclusions that can be drawn from these data.

(1) Within errors, the rate constants are independent of N_2 (or Ar) moderator pressure in the range ~ 400 – 1100 Torr over the whole temperature range studied, and particularly at the lowest temperatures. This strongly suggests that any O_2 dimer formation mediated by third-body collisions in the gas at these temperatures³⁵ is of negligible importance. Indeed, if anything, k_D exhibits a tendency towards higher values at the higher pressures. It is assumed that $(O_2)_2$ in the gas phase is diamagnetic, corresponding to antiferromagnetic coupling in the calculation of Ref. 31.

(2) Based on the measurements of Mu relaxation in the presence of added Al foil (open circles in Fig. 3), there appears to be a small effect of either O_2 dimers formed on the walls of the target vessel (which may then diffuse slowly back into the gas), and/or of O_2 surface adsorption at temperatures $\lesssim 120$ K. Both would have the effect of reducing the concentration of paramagnetic O_2 in the re-

action region, giving rise to a reduced rate constant, which could explain the apparent dip in $\bar{\sigma}_D(T)$ seen in Fig. 3 (reported before as well¹⁹). However, in agreement with the off-line tests mentioned earlier, there was a much smaller change seen at low temperatures than the fivefold change in surface area would indicate. Indeed, the O_2 was present in the ~ 1 atm N_2 moderator at only the 1000-ppm level, and it seems reasonable to expect the surface adsorption isotherms of O_2 and N_2 to be very similar.³⁶ Nevertheless, we cannot rule out the possibility of preferential O_2 adsorption and/or (diamagnetic) O_2 dimer formation at low temperatures on the walls of our target vessel, at the few-percent level.

(3) Within experimental error, the thermally averaged depolarization cross sections $\bar{\sigma}_D(T)$ can be taken as independent of temperature in the range ~ 120 – 500 K, $\bar{\sigma}_D(T) = 3.4 \pm 0.3 \text{ \AA}^2$, regardless of the addition of Al foil. Being temperature independent, this value may also be interpreted as the microscopic cross section $\sigma_D(E)$. Consistent with the aforementioned slopes of $\log k$ versus $\log T$, though, a somewhat better fit to the data in this temperature region can be obtained by allowing for a slight T dependence, $\bar{\sigma}_D(T) = a + bT$, giving fitted values of $a = 3.2 \pm 0.2 \text{ \AA}^2$ and $b = 1.0 \times 10^{-3} \text{ \AA}^2 \text{ K}^{-1}$ from Fig. 3. At the lower temperatures, in the range ~ 88 – 120 K, $\bar{\sigma}_D(T) = 2.9 \pm 0.2 \text{ \AA}^2$, again seemingly independent of temperature over this small range. Recognizing the likelihood that there has been a few-percent decrease in relaxation rate at these temperatures due to surface adsorption effects, one could say that $\bar{\sigma}_D(T)$ for $Mu + O_2$ spin exchange is a smooth and slightly increasing function of temperature over the whole range studied, 88 – 500 K. It is noted that, within errors, a qualitatively similar temperature dependence has been seen in H-H spin-exchange scattering,⁶ the only other reported study of spin exchange over the same temperature range as the data reported herein.

IV. THEORY

The basis for a measurement of electron spin exchange is provided by Eq. (12), where it is assumed that there is no interaction between spin and orbital angular momenta. Consequently, spin-spin coupling ($\sigma_{Mu} \cdot \sigma_{O_2}$) provides the *only* mechanism for spin exchange, and the scattering can then be described in terms of independent phase shifts: quartet ($S = \frac{3}{2}$) and doublet ($S = \frac{1}{2}$) in the present context. Experimental verification of this assumption is provided by the fact that no significant relaxation is seen in $Mu + N_2(^1\Sigma_g^+)$ collisions in the moderator (small λ_0) or in the corresponding H + N_2 spin-scattering experiment.⁸ In these cases the direct spin-exchange cross section is zero (spin-0 molecule).

In a scattering encounter of two like ($s = \frac{1}{2}$) electrons, $|\alpha(1)\alpha(2)\rangle$ is an ($S = 1$) eigenstate of $\sigma_1 \cdot \sigma_2$, and thus is stationary in time. In an encounter of unlike spins, however, the product $|\alpha(1)\beta(2)\rangle$ is a superposition of $|S = 1, M = 0\rangle$ and $|S = 0, M = 0\rangle$ eigenstates, exactly as in the situation leading to muon depolarization in free muonium [Eqs. (2)–(4)]. The large energy difference between those states ($\gtrsim 1$ eV, determined principally by the

Coulomb-like interaction, V_C) causes a rapid evolution of electron spin during the $\sim 10^{-15}$ -s duration of the encounter, leading to $|\beta(1)\alpha(2)\rangle$, as if the spin projections were exchanged. In the case of Mu (or H) + O₂, the spin states are more complicated due to the $S=1$ nature of the O₂ molecule. Again, though, an encounter of like electrons $|\alpha(1)\alpha(2)\alpha(3)\rangle$ is an ($S=\frac{3}{2}$) eigenstate of $\sigma_{\text{Mu}} \cdot \sigma_{\text{O}_2}$ [Eq. (14)], whereas, for example, $|\alpha(1)\beta(2)\beta(3)\rangle$ is not [recall Eq. (15)]. This latter state can be written as a superposition of $|S=\frac{3}{2} M=-\frac{1}{2}\rangle$ and $|S=\frac{1}{2} M=-\frac{1}{2}\rangle$ eigenstates and correspondingly will evolve in time, emerging as the linear combination $|\beta(1)\alpha(2)\beta(3)\rangle + |\beta(1)\beta(2)\alpha(3)\rangle$ from Eq. (14). In both cases, it is an electron pair spin-flip that is promoted by the interaction.

The corresponding exchange cross sections have been treated theoretically by several authors, albeit primarily for the case of $s=\frac{1}{2}$ encounters.^{1-3,14,15} For the case of interest here, Mu(H)+O₂, the spin-flip cross section can be defined in a similar manner, but in terms of the independent phase shifts f_4 and f_2 for quantum scattering from quartet ($S=\frac{3}{2}$) and doublet ($S=\frac{1}{2}$) potentials,

$$\begin{aligned} \sigma_{\text{SF}}(E) &= \frac{1}{4} \int d\Omega |f_4 - f_2|^2 \\ &= \frac{\pi}{k^2} \sum_{l=0}^{\infty} (2l+1) \sin^2(\delta_l^{(4)} - \delta_l^{(2)}) \\ &= \frac{\pi}{k^2} \sum_{l=0}^{\infty} (2l+1) \sin^2 \Delta_l. \end{aligned} \quad (18)$$

It is noted that it is the *difference* between quartet and doublet phase shifts, Δ_l , that is responsible for spin (flip) exchange (the exchange of like spins having undefined cross section in this definition). Classically, this difference can be interpreted as a phase angle through which the spins rotate during the collision, as a result of the energy difference between $S=\frac{1}{2}$ and $\frac{3}{2}$ eigenstates. At distances of a few angstroms, $\Delta_l \rightarrow 0$, so that spin exchange can be a sensitive measure of the intermediate or even short-range nature of the interaction potential.

As in previous H-atom maser⁵⁻⁷ and stored atomic-beam studies,⁸ spin-exchange cross sections are not directly determined in μSR , but instead are found from measured *relaxation* rates in a bulk kinetic experiment. Indeed, with few exceptions, atomic spin-exchange cross sections in general have been determined in "bulk" experiments² rather than in beam experiments, and hence are given as the thermal average $\bar{\sigma}_{\text{SF}} [\equiv \bar{\sigma}_{\text{SF}}(T)]$. This neces-

sitates an evaluation of the time dependence of the density matrix for reacting Mu atoms, ρ_{Mu} , which is under study.³² It appears, though, that an expression for $d\rho/dt$ for the Mu + O₂ reaction can be written in the form given by Balling, Hanson, and Pipkin³⁷ (BHP) for the analogous H-atom reaction [their Eq. (23)], but defined in terms of the spin-projection operators for $S=1$ O₂,

$$\begin{aligned} P_2 &= \frac{1}{6}(2 - \sigma_{\text{Mu}} \cdot \sigma_{\text{O}_2}), \\ P_4 &= \frac{1}{6}(4 + \sigma_{\text{Mu}} \cdot \sigma_{\text{O}_2}). \end{aligned} \quad (19)$$

The use of spin-projection operators obviates cumbersome antisymmetrization of three-electron spin states. This yields,¹⁸ for the *real* parts of $d\rho/dt$, upon substituting the definitions in Eq. (19) above, and invoking the appropriate definitions for the quartet and doublet scattering amplitudes from Eq. (18), the expression

$$\begin{aligned} \frac{d\rho_{\text{Mu}}}{dt} &= \frac{1}{9} \bar{v} n_{\text{O}_2} \bar{\sigma}_{\text{SF}} \text{Tr}_{\text{O}_2} (-8\rho + \sigma_{\text{Mu}} \cdot \sigma_{\text{O}_2} \cdot \rho + \rho \cdot \sigma_{\text{Mu}} \cdot \sigma_{\text{O}_2} \\ &\quad + \sigma_{\text{Mu}} \cdot \sigma_{\text{O}_2} \cdot \rho \cdot \sigma_{\text{Mu}} \cdot \sigma_{\text{O}_2}), \end{aligned} \quad (20)$$

where \bar{v} is defined in Eq. (17), n_{O_2} is the number density of O₂ molecules, Tr_{O_2} indicates a trace over the (unpolarized) O₂ spin coordinates, and $\bar{\sigma}_{\text{SF}}$ represents the thermally averaged spin-flip cross section of interest [see Eq. (24)]. The imaginary terms, which we neglect here, in principle give rise to a shift in the frequency of ω_{Mu} .^{2,37} However, this shift is likely not measurable on the μSR time scale and anyway is expected to be zero for unpolarized electrons.^{32,37} As noted above, the spin-exchange interaction $\sigma_{\text{Mu}} \cdot \sigma_{\text{O}_2}$ can be written in a 9×9 matrix representation of the $|FM_F\rangle$ hyperfine states of triplet muonium and the triplet (ground state) electron spin of the O₂ molecule. It has been given earlier by Berg for the corresponding H-atom study.⁵

Since in the present work the O₂ is unpolarized, the linear terms in Eq. (20) vanish upon taking the trace. Moreover, tracing over $(\sigma_{\text{O}_2})^2 \rho$ gives a factor $\frac{8}{3}$ for unpolarized O₂, so that one is left with the very simple result

$$\frac{d\rho_{\text{Mu}}}{dt} = \frac{8}{27} \bar{v} n_{\text{O}_2} \bar{\sigma}_{\text{SF}} (-3\rho_{\text{Mu}} + \sigma_{\text{Mu}} \cdot \rho \cdot \sigma_{\text{Mu}}). \quad (21)$$

The matrix elements of $\dot{\rho}_{\text{Mu}}$ from Eq. (21) are given in Eq. (22) below, using the notation $1=|11\rangle$, $2=|10\rangle$, $3=|1-1\rangle$, and $4=|00\rangle$ for the $|FM_F\rangle$ hyperfine states of the Mu atom:

$$\frac{d\rho}{dt} = R \begin{array}{c} (1) \\ (2) \\ (3) \\ (4) \end{array} \begin{array}{c} (1) \quad (2) \quad (3) \quad (4) \\ \left[\begin{array}{cccc} -2\rho_{11} + \rho_{22} & -3\rho_{12} & 0 & -3\rho_{14} \\ +\rho_{44} & & & \\ -3\rho_{21} & -3\rho_{22} + \rho_{44} & -3\rho_{23} & -3\rho_{24} \\ & +\rho_{11} + \rho_{33} & & \\ 0 & -3\rho_{32} & -2\rho_{33} + \rho_{22} & -3\rho_{34} \\ & & +\rho_{44} & \\ -3\rho_{41} & -3\rho_{42} & -3\rho_{43} & -3\rho_{44} + \rho_{22} \\ & & & +\rho_{11} + \rho_{33} \end{array} \right] \end{array}, \quad (22)$$

where $R = \frac{8}{27} \bar{v} n_{\text{O}_2} \bar{\sigma}_{\text{SF}}$ from Eq. (21).

The elements of this matrix are identical with those given by BHP (Table VII) for unpolarized electrons, assuming that the off-diagonal contributions are either rapidly oscillating at frequencies comparable to the hyperfine interaction (4463 MHz for Mu), and are thus set to zero, or they contain several terms of comparable magnitude but with opposite signs that are then assumed to cancel.¹⁸ This appears to be a frequent assumption in the literature^{5,29,37,38} and one that we are currently checking in detailed calculations for the μSR case.³²

In μSR , the amplitudes in Eq. (22) that contribute to the time-dependent muon polarization are $\dot{\rho}_{11} - \dot{\rho}_{33} = -2(\rho_{11} - \rho_{33})$ in a weak magnetic field.³² Since this can be expressed by a single relaxation rate, we can compare the integrated form of $d\rho/dt$ directly with the μSR expression for Mu precession in Eq. (1); i.e.,

$$\rho_{\text{Mu}}(t) = \rho_0 e^{-(16/27)\bar{v}n_{\text{O}_2}\bar{\sigma}_{\text{SF}}t} = P_{\text{Mu}} e^{-\lambda_D t}. \quad (23)$$

Thus since the experimental depolarization rate $\lambda_D = n_{\text{O}_2} \bar{v} \bar{\sigma}_D$ from Eqs. (16) and (17), we have the result $\bar{\sigma}_{\text{SF}} \equiv \bar{\sigma}_{\text{SF}}(T) = \frac{27}{16} \bar{\sigma}_D(T)$. The same factor appears in a longitudinal field of arbitrary strength (given, however, as $\frac{27}{32}$ by Mobley²⁹), but then the experimental relaxation rate is also field dependent [recall Eq. (5)].^{29,32} In a transverse field of arbitrary strength, two or more frequency components are seen [recall Eq. (7)], which may relax with different rates.³² It can be remarked that in the case of weak field spin exchange with spin- $\frac{1}{2}$ molecules (e.g., Mu-NO), the relationship between the experimental spin-flip and μSR depolarization cross sections is simply $\bar{\sigma}_{\text{SF}}(T) = 2\bar{\sigma}_D(T)$, as expected from the previous discussion and also from Table VII in BHP.

In previous publications, slightly different coupling factors had been assumed;^{18,19} specifically, $\bar{\sigma}_{\text{SF}}(T) = 2f\bar{\sigma}_D(T)$, where the factor of 2 was to account for the statistical fraction of “spin-down” (β) electrons in the gas, and f was assumed to arise from the off-diagonal elements of $d\rho/dt$. For O_2 ($S=1$), this assumption gives $f = \frac{9}{8}$, as can be seen from Eq. (22), whereas for NO ($S = \frac{1}{2}$), $f = \frac{4}{3}$, from Table VII in BHP. Current calculations³² demonstrate that this procedure was not correct for the transverse-field μSR geometry of interest ($f = \frac{27}{32}$ for O_2), the earlier reported values for $\bar{\sigma}_{\text{SF}}(T)$ being then about 30% too high in each case.¹⁸

V. DISCUSSION

A. Comparison with theory

Table II compares the experimental and theoretical¹⁶ values of $\bar{\sigma}_{\text{SF}}(T)$ for Mu+ O_2 . The experimental results are found from the definition in Eq. (23); i.e., $\bar{\sigma}_{\text{SF}}^{\text{exp}}(T) = \frac{27}{16} \bar{\sigma}_D(T)$, with the latter values given in Table I, but taken only from the data in the absence of added Al [i.e., entries in the part (a) of the table]. As noted above, the experimental cross sections ($\bar{\sigma}_{\text{SF}}$) given here are about 30% lower than those reported earlier over a

TABLE II. Comparison of theoretical and experimental thermal spin-flip cross sections ($\bar{\sigma}_{\text{SF}}$) for Mu+ O_2 .

T (K)	$\bar{\sigma}_{\text{SF}}^{\text{exp}}(T)^a$	$\bar{\sigma}_{\text{SF}}(\text{FA})^b$	$\bar{\sigma}_{\text{SF}}(\text{SI})^c$
88	4.95±0.16	6.00	11.0
100	4.95±0.15	6.57	12.04
108	4.85±0.15	7.00	12.7
118	5.10±0.18	7.50	13.5
128	5.73±0.21	8.00	14.3
135	5.78±0.16	8.40	14.7
176	5.67±0.16	10.5	18.0
188	5.61±0.12	11.1	19.0
217	5.73±0.22	12.5	20.7
295	5.78±0.15	16.2	24.6
338	6.00±0.44	18.0	26.6
405	6.30±0.40	20.9	28.9
500	6.30±0.45	24.74	32.12

^aExperimental thermally averaged spin-exchange cross sections from the definition in Eq. (23), in units of 10^{-16} cm^2 . The 295-K value is a weighted average of the room-temperature values from Table I.

^bFrom the theoretical calculations reported to us by Laganà (Ref. 16) (in units of 10^{-16} cm^2) for the FA interaction, as described in the text. Values other than those at 100 and 500 K were obtained by a linear interpolation from tabulated results.

^cAs in b, but for the SI interaction, described in the text.

similar temperature range, but based on a less complete set of data.^{18,19} At room temperature the value for $\bar{\sigma}_{\text{SF}}^{\text{exp}}(T)$ given in Table II in fact agrees very well with that reported much earlier by Mobley *et al.* in a longitudinal field,²⁹ but is almost a factor of 2 lower than that obtained more recently by Kondow *et al.* using the same technique.³⁹

The theoretical expression for the thermally averaged spin-flip (exchange) cross section follows from the definition in Eq. (17),

$$\bar{\sigma}_{\text{SF}} \equiv \bar{\sigma}_{\text{SF}}(T) = [1/(k_B T)^2] \int_0^\infty \sigma_{\text{SF}}(E) E e^{-E/k_B T} dE, \quad (24)$$

where $\sigma_{\text{SF}}(E)$ is obtained from the partial-wave sum in Eq. (18). See also Ref. 40. The spin-exchange cross sections, $\bar{\sigma}_{\text{SF}}(T)$ for reaction (10) given in Table II, have been calculated by Laganà and co-workers¹⁶ using the largely semiempirical potential of Farantos *et al.* that has been optimized by best fitting of some *ab initio* points to spectroscopic data for the HO_2 radical.¹⁷ While reactive collisions and coupling to vibrational and electronic excitation can be ignored at the temperatures of interest ($\lesssim 500$ K), coupling to rotational states in Mu(H)+ O_2 is expected from an anisotropy in the interaction potential. A complete coupled-channel calculation including all of the approximately 20 J states populated in O_2 at 300 K is a formidable problem, though, and decoupling schemes need to be invoked. The decoupling of spin- and orbital-angular-momentum vectors has already been mentioned. Rotational decoupling in Ref. 16 is accomplished by considering two limiting models for the atom-molecule encounter. When rotational energies are large, the rapidly

rotating molecule presents an essentially spherical image to the incident Mu atom, and any angular dependence in the interaction is averaged out.⁴⁰ This limit is denoted as a spherical interaction (SI) in Table II, and is expected to be most valid at high temperatures. The other limit is provided at low temperatures when the O₂ molecule can be considered at some fixed orientation with respect to the velocity of the incident Mu (H) atom. In this scheme, called a fixed-angle (FA) approximation in Table II [or alternatively as an oriented-frame-decoupling (OFD) scheme¹⁶], the final value of the scattering amplitude (and hence $\bar{\sigma}_{\text{SF}}$) is obtained by integrating over a range of fixed θ . The FA approximation is similar then to infinite-order sudden (IOS) approximations, which have enjoyed considerable success to date in calculations of inelastic cross sections.⁴¹

The overall level of agreement between theory and experiment in Table II is poor. Specifically, the theoretical $\bar{\sigma}_{\text{SF}}(T)$ for both coupling schemes rises much faster with increasing temperature than do the experimental cross sections (Fig. 2). This has also been noted elsewhere.¹⁹ Although it may be fortuitous, at the lowest temperatures and for the FA calculation, the agreement appears quite acceptable, theory being only about 20% too high. However, at 500 K the level of disagreement becomes a factor of 4 for the FA approximation and a factor of 5 for the SI approximation. Indeed, the trend in the calculations to successively larger cross sections with increasing T is hard to understand. One would expect to see a decrease in $\bar{\sigma}_{\text{SF}}(T)$ at the highest temperatures, from Eq. (24), seen also in other theoretical calculations of thermal spin-exchange cross sections.^{14,15}

Despite the poor agreement between theory and experiment apparent from the overall comparisons in Table II, there is nevertheless support for the earlier remark that Mu-O₂ spin exchange is sensitive to differences in the intermolecular potential, in contrast to the corresponding H-O₂ reaction.¹⁶ Even at the lowest temperatures, where the FA cross sections are only 20% too high, the SI ones are too large by over a factor of 2, due to enhanced resonant capture at specific energies of this very light atom. This is typical of spherical interactions. Other examples are provided by comparisons of theoretical cross sections for Mu-H and H-H spin exchange,¹⁴ and He⁺-H and H-H spin exchange.⁴² In molecular scattering though, the effect of resonant enhancement in scattering cross sections tends to be reduced by molecular anisotropy and rotational averaging, as in the FA (OFD) calculation of Ref. 16. On the other hand, as noted, the FA approximation is essentially an IOS one, valid for short-range (repulsive) interactions,⁴¹ but it is not at all clear that it is appropriate for the quasielastic spin-exchange process. Moreover, the IOS approximation itself is inherently an "energy sudden" approximation, in which the collision energy is expected to be much greater than those of internal (rotational) degrees of freedom; again, it is not clear that this approximation is valid at thermal energies in a bulk kinetic experiment.

In order to be able to assess further whether it is the (isotopically invariant) HO₂ potential surface itself, or approximations to the atom-molecule interaction on that

surface which are at the root of the disagreement between theory and experiment cited above, it is necessary to have the spin-exchange calculations repeated with different potentials²⁰⁻²³ than the parametrized form of Farantos *et al.*¹⁷ utilized in Ref. 16. As noted earlier, the Melius and Blint potential surface,²⁰ which is similar to the more recent one of Dunning *et al.*,²¹ gives a reasonably good account of the reactive channel (8) for H atoms.²⁴ These are also "global" surfaces, in contrast to the "local" one of Ref. 17, which has been optimized in regions near the equilibrium geometry of the HO₂ radical. This could have important implications for dynamical calculations. In addition, these newer potential surfaces have a small (~0.1 eV) barrier in the entrance channel, which could result in reduced cross sections for Mu+O₂ in comparison with those calculated on a surface with no barrier,¹⁶ since relatively few partial waves are involved at the temperatures of interest. Indeed, at the lowest temperatures, further decreases in cross section could result, consistent with the aforementioned trend in the data (Fig. 3). However, the role played by tunneling of the light mass Mu atom will have to be assessed. If this is at all significant, it can be expected to be much more pronounced for Mu than for the corresponding H-atom reaction.

B. Comparison with H-atom data

It is well known that measurements of isotopic mass effects provide valuable experimental tests of our understanding of chemical reaction dynamics for reactive scattering, but it has not heretofore been established whether a similar sensitivity is to be found for quasielastic scattering in the study of spin-exchange cross sections. Although there are some theoretical calculations,^{14,16,42} there are no comparisons of experimental spin-exchange cross sections over a wide range of temperature and isotopic mass, other than those reported here.

The H+O₂ spin-exchange cross sections have been measured by Berg⁵ and by Gordon *et al.*⁷ in H-atom maser experiments, and more recently by Anderle *et al.* using a stored atomic beam technique.⁸ Unfortunately, there is considerable uncertainty in the reported values for these cross sections. The maser experiment either monitors the change in amplitude of the signal, manifest by the population difference $\rho_{22} - \rho_{44}$ of the matrix of Eq. (22), giving $\lambda_1 = 1/T_1 = 4R$, or the relaxation of the oscillating hyperfine component, manifest by the off-diagonal element ρ_{24} , giving $\lambda_2 = 1/T_2 = 3R$. Note that $T_2/T_1 = \frac{4}{3}$ (Ref. 5). Gordon *et al.* report experimental spin-"exchange" cross sections at 310 K of $8.8 \pm 0.7 \text{ \AA}^2$, but confuse this considerably with another value given in the text of their paper, which is larger by essentially a factor of 2 (or possibly $2 \times \frac{9}{8}$), which seemingly has its origin in a definition of spin exchange that includes equal contributions from the exchange of like ($\alpha\alpha$) and unlike ($\alpha\beta$) spins. Berg clearly quotes values for $\bar{\sigma}_{\text{SF}}$, but his number is about twice as large as the smaller value quoted by Gordon *et al.* (this is also true in the case of H+NO). On the other hand, it agrees well with their larger value. Gordon *et al.* do not appear to have taken account of the correct angular-momentum coupling factors in the densi-

ty matrix, which was one of the principal points of Berg's paper. It would certainly be advantageous to the field to have the H-maser experiments repeated.

It is not clear to us just how to interpret the experiment of Anderle *et al.*⁸ As in the H-maser experiment, the hyperfine states $|1\rangle$ and $|2\rangle$ of the H atom are selected by sextupole focusing and are passed through a reaction cell (containing O₂ or NO), but then are refocused through a second sextupole onto a bolometer detector, either in the presence (which removes state $|1\rangle$) or absence of a RF pulse. Our understanding is that this experiment actually counts populations directly, whereas the H-maser experiment either monitors differences in populations (T_1) or relaxation (T_2), as in the μ SR experiment. The H-maser and μ SR experiments actually sample different elements of the complete density matrix.³² Anderle *et al.* quote "depolarization" cross sections at room temperature ($10 \pm 1 \text{ \AA}^2$) that they identify as $\bar{\sigma}_{\text{SF}}$, and which are in good agreement with the apparently accepted (lower) values of Gordon *et al.* ($8.8 \pm 0.7 \text{ \AA}^2$). However, they also appear not to have properly considered the elements of the density matrix and we are suspicious that measured relaxation rates in these two different types of experiments cannot be directly compared.³² There is clearly a complicated time dependence to the amplitudes $\dot{\rho}_{ii}$ from Eq. (22), so that an additional factor of 2 in their relaxation rates may not be unexpected. If so, all the above-stated H-O₂ measurements would be brought into line, with an average room-temperature cross section of $\sim 20 \text{ \AA}^2$ for $\bar{\sigma}_{\text{SF}}(\text{H})$.

Table III compares the reported thermal spin-flip (exchange) cross sections for H+O₂ from the data of Refs. 7 and 8 with the present μ SR values from Table II. As noted, there is some uncertainty as to which numerical factors are necessary for a correct interpretation of the relaxation rates in the different H-atom experiments,³² but for now we assume the reported experimental "depolarization"

cross sections are, as stated by the authors, essentially the same as the spin-flip cross section of interest, $\bar{\sigma}_{\text{SF}}$. We suspect that the correct values may be even higher.³² The higher-temperature values for $\bar{\sigma}_{\text{SF}}(\text{H})$ are those of Gordon *et al.*⁷ Unfortunately, these have been measured at only a few temperatures just above 300 K, meaning that $\bar{\sigma}_{\text{SF}}(\text{H})$ and $\bar{\sigma}_{\text{SF}}(\text{Mu})$ can be compared over only a rather restricted range of temperatures. The theoretical values for $\bar{\sigma}_{\text{SF}}(\text{H})$ and $\bar{\sigma}_{\text{SF}}(\text{Mu})$ from the FA calculations of Laganà and co-workers are also given in Table III. There is a significant isotope effect seen in the data [$\bar{\sigma}_{\text{SF}}(\text{H}) \sim 1.5 \bar{\sigma}_{\text{SF}}(\text{Mu})$] which tends to decrease with increasing temperature from a ratio of ~ 1.7 at 295 K to ~ 1.3 at 390 K. It should be recalled that these ratios are about 30% higher than those given earlier, leading to the statement then that there was little or no isotope effect seen in comparisons of Mu-O₂ and H-O₂ spin-exchange cross sections.^{9,18} As mentioned earlier, this difference in emphasis is due to the correspondingly differing numerical factors affecting the μ SR spin-exchange relaxation rates in evaluating $d\rho/dt$.³²

The (FA) calculations of Laganà and co-workers¹⁶ do indicate that $\bar{\sigma}_{\text{SF}}(\text{H}) > \bar{\sigma}_{\text{SF}}(\text{Mu})$, although the effect is only $\sim 20\%$, at most, not a factor of almost 2. On the other hand, the calculated cross-section ratio $\bar{\sigma}_{\text{SF}}(\text{H})/\bar{\sigma}_{\text{SF}}(\text{Mu})$ does tend to fall off slightly with increasing temperature, in agreement with the trend in the data. It has already been noted that the principal failure in the theory¹⁶ lies in the absolute magnitude of the calculated cross sections.

The essentially temperature-independent Mu-O₂ (and H-O₂) experimental cross sections can be simplistically understood within the random-phase approximation (RPA) to Eq. (18),¹⁸ in which the difference in phase shifts, $\sin^2\Delta_l$, is assumed to average to a value of $\frac{1}{2}$ up to some "cutoff" partial wave l_c , beyond which they average to zero. Thus, in the RPA, Eq. (18) can be written as

$$\sigma_{\text{SF}}(\text{RPA}) \simeq \frac{\pi}{2k^2} \sum_{l=0}^{l_c} (2l+1) \simeq \frac{\pi}{2k^2} (l_c+1)^2. \quad (25)$$

Implicit in Eq. (25) is the assumption that enough partial waves contribute to the sum so that one can meaningfully speak of an average phase shift. Since l_i is proportional to μ_i , where μ_i is the reduced mass of colliding partners for the i th partial wave, this is likely to be a much better approximation for H-O₂ than for Mu-O₂ scattering (where $\mu_{\text{Mu}} \approx \frac{1}{5}\mu_{\text{H}}$). At high enough temperatures (energies), in the limit where $l_c \gg 1$, Eq. (25) predicts that σ_{SF} would be both temperature *and* mass independent.¹⁸ At the temperatures of interest in these experiments, however, corresponding to average energies $\lesssim 0.05$ eV, relatively few partial waves contribute. Structure in the cross section in the low momentum region¹⁶ where l_c is small dictates that $\sin^2\Delta_l$ is likely not random, particularly for Mu-O₂.

That the RPA is in fact likely a poor approximation for Mu can be seen from Fig. 4, which plots the partial cross sections σ_l from the calculation of Ref. 16 for Mu (triangles, top scale) and H (circles, bottom scale) versus

TABLE III. Comparison of H-O₂ and Mu-O₂ thermal spin-flip cross sections ($\bar{\sigma}_{\text{SF}}$).

Reaction	T (K)	$\bar{\sigma}_{\text{SF}}^{\text{exp}}(T)^a$ (10^{-16} cm^2)	$\bar{\sigma}_{\text{SF}}(\text{FA})^b$
Mu + O ₂	295	5.78 ± 0.15	16.2
Mu + O ₂	338	6.00 ± 0.44	18.0
Mu + O ₂	405	6.30 ± 0.40	20.9
Mu + O ₂	500	6.30 ± 0.45	24.7
H + O ₂	295	10 ± 1	18.8
H + O ₂	310	8.8 ± 0.7	19.0
H + O ₂	315	9.8 ± 1.0	19.2
H + O ₂	350	8.3 ± 0.7	22.3
H + O ₂	388	8.0 ± 0.7	24.6

^aExperimental thermally averaged spin-flip cross sections for Mu+O₂ (Table II) and H+O₂ (Refs. 7 and 8), in units of 10^{-16} cm^2 . See discussion in the text.

^bThe theoretical calculation of $\bar{\sigma}_{\text{SF}}(\text{Mu})$ and $\bar{\sigma}_{\text{SF}}(\text{H})$ from the FA calculations of Laganà and co-workers (Ref. 16).

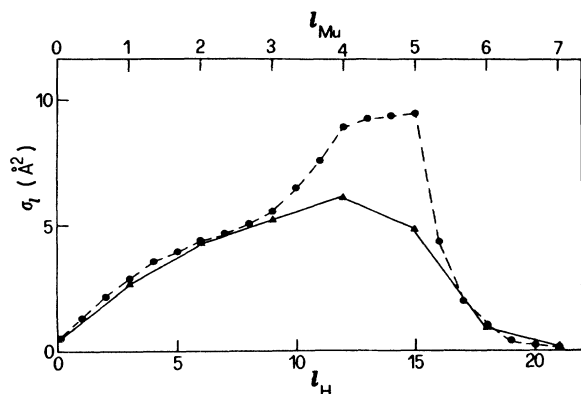


FIG. 4. Partial-wave spin-exchange cross sections, σ_l for $\text{Mu}+\text{O}_2$ (l_{Mu} , triangles, top scale) and $\text{H}+\text{O}_2$ (l_{H} , circles, bottom scale) from the calculation of Ref. 16.

l . For $\text{Mu}+\text{O}_2$, $l_{\text{max}} \approx 4$, whereas it is ≈ 14 for $\text{H}+\text{O}_2$. In terms of an interaction time, if Δ_l can be assumed to be $\propto 1/v$, then for $\Delta_l \ll 1$, $\sin^2 \Delta_l \propto 1/v^2$, which is then directly proportional to the reduced mass μ at a given energy. From such elementary considerations it is clear that something like a factor-of-2 reduction in thermal spin-exchange cross sections of Mu relative to H could well be expected.²⁹ The present experimental comparison is certainly consistent with this, particularly in view of the uncertainties in the extraction of $\bar{\sigma}_{\text{SF}}$ from the H-atom data in Refs. 5, 7, and 8. This assessment is also in accord with theoretical calculations comparing He^+-H and H-H spin exchange.⁴² Although the interaction potential in the case of He^+-H contains a long-range contribution, this does not appear to play a big role in the calculation of $\bar{\sigma}_{\text{SF}}$, particularly at higher temperatures. Large isotope effects are seen with $\bar{\sigma}_{\text{SF}}(\text{He}^+-\text{H}) > \bar{\sigma}_{\text{SF}}(\text{H}-\text{H})$, although these species differ in reduced mass by only a factor of 1.6.

Finally, it is worth comparing the present experimental results for $\text{Mu}-\text{O}_2$ spin exchange with those of Desaintfuscién and Audoin for H-H,⁶ which, as noted, to

our knowledge, are the only experimental results in H-atom spin exchange to cover the same temperature range as the present ones for $\text{Mu}-\text{O}_2$. Although seemingly even less dependent on temperature, the H-H cross sections qualitatively exhibit the same trend in $\sigma_{\text{SF}}(T)$ with temperature as the present results for $\text{Mu}-\text{O}_2$, but the absolute magnitude of the latter is about 4 times smaller; e.g., near room temperature, $\bar{\sigma}_{\text{SF}}^{\text{exp}} \sim 6 \times 10^{-16} \text{ cm}^2$ for $\text{Mu}-\text{O}_2$, versus $\sim 23 \times 10^{-16} \text{ cm}^2$ for H-H spin exchange. This is a somewhat surprising result since one would expect the number of partial waves to be similar in both cases. On the other hand, the reduced masses are different. Since H-H spin exchange can only be due to a spherical interaction, the much reduced cross section seen for $\text{Mu}-\text{O}_2$ (and $\text{H}-\text{O}_2$) may be an indication of the importance of anisotropy and rotational couplings in the atom-molecule potential. In this case one may expect, in agreement with the FA calculation of Laganà and co-workers comparing $\text{Mu}-\text{O}_2$ and $\text{H}-\text{O}_2$ spin exchange,¹⁶ that the enhanced velocity of Mu relative to H ($\bar{v}_{\text{Mu}} \approx 3\bar{v}_{\text{H}}$) would mean a correspondingly shortened interaction time, so that Mu may indeed be affected by specific orientations of the O_2 molecule, while the H atom would be affected by a spherical orientation. To echo our earlier remarks though, additional theoretical calculations on newer potential surfaces are clearly required.

ACKNOWLEDGMENTS

We would like to thank sincerely Dr. Antonio Laganà for providing us with tables of the spin-exchange cross sections and particularly for providing us with Fig. 4, from Ref. 16. We would also like to thank Professor R. F. Snider for his many helpful comments and his critical reading of the manuscript. Helpful discussions with Professor G. Scoles and Professor W. Happer are also acknowledged. One of us (D.G.F.) also thanks the Canada Council for support through a Killam research fellowship. The continuing financial support of the Natural Science and Engineering Research Council (Canada) is also gratefully acknowledged.

*Present address: Physikalisch-Chemisches Institut der Universität Zürich, Winterthurestrasse 190, CH-8057, Switzerland.

¹H. S. W. Massey, E. H. S. Burhop, and H. A. Gilbody, *Electronic and Ionic Impact Phenomena*, 2nd ed. (Oxford University Press, London, 1971), Vol. III; A. Dalgarno, Proc. R. Soc. London, Ser. A **262**, 132 (1961).

²W. Happer, Rev. Mod. Phys. **44**, 169 (1972).

³D. R. Swanson, D. Tupa, and L. W. Anderson, J. Phys. B **18**, 4433 (1985); H. R. Cole and R. E. Olson, Phys. Rev. A **31**, 2137 (1985).

⁴T. E. Chupp and K. P. Coulter, Phys. Rev. Lett. **55**, 1074 (1985); X. Zeng, Z. Wu, T. Call, E. Mivon, D. Schreiber, and W. Happer, Phys. Rev. A **31**, 260 (1984); N. D. Bhaskar, W. Happer, and T. McClland, Phys. Rev. Lett. **49**, 25 (1982).

⁵H. C. Berg, Phys. Rev. **137**, A1621 (1965).

⁶M. Desaintfuscién and C. Audoin, Phys. Rev. A **13**, 2070 (1976).

⁷E. B. Gordon, B. I. Ivanov, A. P. Perminov, A. N. Ponomarev, V. L. Tal'roze, and S. G. Khidirov, Pis'ma Zh. Eksp. Teor. Fiz. **17**, 548 (1973) [JETP Lett. **17**, 395 (1973)].

⁸M. Anderle, D. Bassi, S. Iannotta, S. Marchetti, and G. Scoles, Phys. Rev. A **23**, 34 (1981).

⁹D. G. Fleming, in *Proceedings of the Twelfth International Conference on the Physics of Electronic and Atomic Collision, Gatlinburg, 1982*, edited by S. Datz (North-Holland, Amsterdam, 1982), p. 297; D. G. Fleming, D. M. Garner, and R. J. Mikula, Hyperfine Interact. **8**, 337 (1981).

¹⁰I. D. Reid, D. M. Garner, L. Y. Lee, M. Senba, D. J. Arseneau, and D. G. Fleming, J. Chem. Phys. **86**, 5578 (1987).

¹¹E. Roduner, Prog. React. Kinet. **14**, 1 (1986); D. C. Walker, *Muons and Muonium in Chemistry* (Cambridge University

- Press, Cambridge, England, 1983).
- ¹²A. Wagner, R. Duchovic, R. E. Turner, D. M. Garner, and D. G. Fleming (unpublished).
- ¹³S. G. Redsun, R. J. Knize, G. D. Cates, and W. Happer, *Bull. Am. Phys. Soc.* **33**, 973 (1988).
- ¹⁴B. Shizgal, *J. Phys. B* **12**, 3611 (1979); A. J. Berlinsky and B. Shizgal, *Can. J. Phys.* **58**, 881 (1980).
- ¹⁵A. C. Allison, *Phys. Rev. A* **5**, 2695 (1972); A. C. Allison and A. Dalgrano, *Astrophys. J.* **158**, 423 (1969).
- ¹⁶V. Aquilanti, G. Grossi, and A. Laganà, *Hyperfine Interact.* **8**, 347 (1981); A. Laganà (unpublished); and private communication.
- ¹⁷S. Farantos, E. C. Leisegang, J. N. Murrell, K. Sorbie, J. J. C. Teixeira-Dias, and A. J. C. Varandas, *Mol. Phys.* **34**, 947 (1977).
- ¹⁸R. J. Mikula, Ph.D. thesis, University of British Columbia, 1981; R. J. Mikula, D. M. Garner, and D. G. Fleming, *J. Chem. Phys.* **75**, 5362 (1981); D. G. Fleming, R. J. Mikula, and D. M. Garner, *ibid.* **73**, 2751 (1980).
- ¹⁹M. Senba, D. M. Garner, D. J. Arseneau, and D. G. Fleming, *Hyperfine Interact.* **17-19**, 703 (1984).
- ²⁰C. F. Melius and R. J. Blint, *Chem. Phys. Lett.* **64**, 183 (1979).
- ²¹T. H. Dunning, Jr., S. P. Walch, and M. M. Goodgame, *J. Chem. Phys.* **74**, 3482 (1981).
- ²²S. R. Langhoff and R. L. Jaffee, *J. Chem. Phys.* **71**, 1473 (1979).
- ²³W. J. Lemon and W. L. Hase, *J. Phys. Chem.* **91**, 1596 (1987).
- ²⁴K. Kleinermanns and R. Schinke, *J. Chem. Phys.* **80**, 1400 (1984); K. Kleinermanns and J. Wolfrum, *ibid.* **80**, 1446 (1984).
- ²⁵M. Senba, *J. Phys. B* **21**, 3093 (1988); D. G. Fleming and M. Senba, in *Atomic Physics with Positrons*, edited by J. W. Humberston and E. A. G. Armour (Plenum, New York, 1987), p. 343; D. G. Fleming, R. J. Mikula, and D. M. Garner, *Phys. Rev. A* **26**, 2527 (1982).
- ²⁶J. L. Beveridge, J. Doornbos, and D. M. Garner, *Hyperfine Interact.* **32**, 907 (1986); J. L. Beveridge, J. Doornbos, D. M. Garner, D. J. Arseneau, I. D. Reid, and M. Senba, *Nucl. Instrum. Methods A* **240**, 316 (1985).
- ²⁷D. G. Fleming, D. M. Garner, L. C. Vaz, D. C. Walker, J. H. Brewer, and K. M. Crowe, *Adv. Chem. Ser.* **175**, 279 (1979); P. W. Percival and H. Fischer, *Chem. Phys.* **16**, 89 (1976); J. H. Brewer, K. M. Crowe, F.N. Gygas, and A. Schenck, in *Positive Muons and Muonium in Matter*, edited by V. W. Hughes and C. S. Wu (Academic, New York, 1975).
- ²⁸E. Rodner and H. Fischer, *Chem. Phys.* **54**, 261 (1981).
- ²⁹R. M. Mobley, Ph.D. thesis, Yale University, 1967; R. M. Mobley, J. J. Amato, V. W. Hughes, J. E. Rothberg, and P. A. Thompson, *J. Chem. Phys.* **47**, 3074 (1967).
- ³⁰C. J. Cobos, H. Hippler, and J. Troe, *J. Phys. Chem.* **89**, 342 (1985); K. J. Hsu, J. L. Durant, and F. Kaufman, *ibid.* **91**, 1895 (1987).
- ³¹A. van der Avoird and G. Brocks, *J. Chem. Phys.* **87**, 5346 (1987); P. E. S. Wormer and A. van der Avoird, *ibid.* **81**, 1929 (1984).
- ³²R. E. Turner, R. F. Snider, and D. G. Fleming (unpublished).
- ³³R. A. Ferrell, *Phys. Rev.* **110**, 1355 (1958).
- ³⁴I. D. Reid, D. M. Garner, D. J. Arseneau, M. Senba, and D. G. Fleming (unpublished).
- ³⁵C. A. Long and G. E. Ewing, *J. Chem. Phys.* **58**, 4824 (1973).
- ³⁶See, e.g., V. Fried, H. F. Hamerka, and U. Blukis, *Physical Chemistry* (Collier MacMillan, New York, 1977), p. 715.
- ³⁷L. C. Balling, R. J. Hanson, and F. M. Pipkin, *Phys. Rev.* **133**, A607 (1964).
- ³⁸J. Vanier, C. Jacques, and C. Audoin, *Phys. Rev. A* **31**, 3967 (1985).
- ³⁹T. Kondow, A. Matsushita, K. Kuchitsu, K. Nishiyama, Y. Morozumi, and K. Nagamine, *Hyperfine Interact.* **32**, 807 (1986).
- ⁴⁰A. E. Glassgold and S. A. Lebedeff, *Ann. Phys. (N.Y.)* **28**, 181 (1964); E. Glassgold, *Phys. Rev.* **132**, 2144 (1963).
- ⁴¹D. J. Kouri, in *Atom-Molecule Collision Theory: A Guide for the Experimentalist*, edited by R. B. Bernstein (Plenum, New York, 1979), Chap. 9.
- ⁴²C. Falcón, L. Opradolce, and R. D. Piacentini, *J. Phys. B* **11**, 3033 (1978).